N O T I C E

THIS DOCUMENT HAS BEEN REPRODUCED FROM MICROFICHE. ALTHOUGH IT IS RECOGNIZED THAT CERTAIN PORTIONS ARE ILLEGIBLE, IT IS BEING RELEASED IN THE INTEREST OF MAKING AVAILABLE AS MUCH INFORMATION AS POSSIBLE

50th Anniversary Celebration

American Institute of Aeronautics and Astronautics
1290 Avenue of the Americas, New York, N.Y. 10104
Telephone 212/581-4300

June 29, 1981

TO: Shirley Peigara

FROM: Norma Brennan, Director, Editorial Department

A back-up paper is enclosed for the following Synoptic:

Author(s): W. H. Hui and Murray Tobak

Title of Synoptic: "Unsteady Newton-Busemann Flow Theory Part II: Bodies of Revolution" (Log No. J12130)

Title of Back-up Paper: Same as above.

Correspondence with: Dr. Murray Tobak
Aerothermodynamics Section
Entry Technology Branch
Attn: STP:234-1
NASA Ames Research Center
Moffett Field, California 94035

Journal: AIAA Journal

Scheduled Issue: October 1981

(Mrs.) Norma Brennan

Enclosure

UNSTEADY NEWTON-BUSEMANN FLOW THEORY

PART II: BODIES OF REVOLUTION

By

W. H. Hui and Murray Tobak

/April 1981/

Backup Document for AIAA Synoptic Scheduled
for Publication in the AIAA Journal, October 1981

NASA Ames Research Center
Aerothermodynamics Section
Entry Technology Branch
Attn: STP:234-1
Moffett Field, CA 94035

UNSTEADY NEWTON-BUSEMANN FLOW THEORY

PART II: BODIES OF REVOLUTION

W. H. Hui* and Murray Tobak†

Ames Research Center, NASA, Moffett Field, California

Abstract

Newtonian flow theory for unsteady flow past oscillating bodies of revolution at very high Mach numbers is completed by adding a centrifugal force correction to the impact pressures. Exact formulas for the unsteady pressure and the stability derivatives are obtained in closed form which require only numerical quadratures of terms involving the body shape. They are applicable to bodies of revolution that have arbitrary shapes, arbitrary thicknesses, and either sharp or blunt noses. The centrifugal force correction arising from the curved trajectories followed by the fluid particles in unsteady flow is shown to be very important. It cannot be neglected even for the case of a circular cone, for which the centrifugal force contribution in steady flow is zero. With the inclusion of this correction the present theory is shown to be in excellent agreement with experimental results for sharp cones and for cones with small nose bluntness; however, the theory gives poor agreement with the results of experiments in air for bodies having moderate or large nose bluntness. Finally, the pitching motions of slender power-law bodies of revolution are shown to be always dynamically stable according to Newton-Busemann theory.

Index categories: Nonsteady Aerodynamics; Supersonic and Hypersonic Flow; Entry Vehicle Dynamics and Control.

*Visiting Professor. Permanently Professor of Applied Mathematics, University of Waterloo, Waterloo, Ontario, Canada.

†Research Scientist. Member AIAA.

I. Introduction

This paper continues the study of unsteady Newton-Busemann flow theory begun by the authors in Part I (Ref. 1) by extending it to cover the case of bodies of revolution as well as airfoils. Specifically, we consider high Mach number flow past a body of revolution of arbitrary thickness and shape having a sharp or blunt nose, which is performing a combined pitching and plunging oscillation of low frequency. The aim is to calculate the resulting unsteady flow on the basis of the Newton-Busemann flow model. In this model we conceive of the surface pressure as being composed of two parts: the Newtonian impact pressure and a centrifugal-force correction owing to the curved trajectories that fluid particles follow along the surface subsequent to their impact. In Sec. II the Newtonian impact pressure is derived, and in Sec. III the trajectories of the fluid particles are determined. These are used in Sec. IV to find the steady and unsteady centrifugal force corrections. In Sec. V these general results are applied to study the dynamic stability of classes of bodies of revolution, including the effects of the unsteady centrifugal force and of nose bluntness. Comparisons with experimental results are also shown, and, finally, conclusions are presented in Sec. VI.

II. Newtonian Impact Pressure

Consider a body of revolution in a uniform hypersonic flow U_∞ which performs a harmonic pitching oscillation with zero mean angle of attack about the pivot axis C. Simultaneously, the pivot axis undergoes a harmonic plunging oscillation, so that the body is in a combined pitching and plunging motion (Fig. 1). The body may have a sharp or blunt nose, but cannot be flat-nosed. Let a fixed system of Cartesian coordinates OXYZ (with corresponding unit vectors denoted by $\hat{I}$, $\hat{J}$, and $\hat{K}$) be such that O is at the mean position of the nose and OX is along the direction of the free stream

U_∞. Let the body-fixed system of Cartesian coordinates $O'xyz$ (with corresponding unit vectors denoted by $\vec{i}$, $\vec{j}$, and $\vec{k}$) be such that O' is at the nose and $O'x$ is along the axis of symmetry of the body. Concurrently, a body-fixed system of cylindrical coordinates (x,r,ϕ) (with corresponding unit vectors denoted as $\vec{i}$, $\vec{e}_r$, and $\vec{e}_\phi$) will be used which is related to (x,y,z) by

$$x = x \ , \qquad y = r\cos\phi \ , \qquad z = r\sin\phi \tag{1}$$

In the following, all the lengths X, Y, Z, x, y, z, r, h, etc., are scaled by the length of the body ℓ, velocities $\vec{v}$ by U_∞, density ρ by ρ_∞, pressure p by $\rho_\infty U_\infty^2$, and the time variable t by ℓ/U_∞. Thus, for example, $\rho_\infty = U_\infty = \ell = 1$.

The harmonic pitching oscillation of the body with frequency ω may be represented by the displacement angle of pitch θ (Fig. 1)

$$\theta(t) = \bar{\theta}\, e^{ikt} \tag{2}$$

where

$$k = \frac{\omega\ell}{U_\infty} \tag{3}$$

is the reduced frequency and $\bar{\theta}$ is the amplitude of oscillation. Likewise, the harmonic plunging oscillation of the body at the same frequency ω may be represented by the linear displacement Y_c (Fig. 1) where

$$Y_c(t) = \bar{Y}_c\, e^{ikt} \tag{4}$$

which is related to the flightpath angle $\gamma(t)$ by

$$\dot{Y}_c(t) = ik\bar{Y}_c\, e^{ikt} \equiv \gamma(t) = \bar{\gamma}\, e^{ikt} \tag{5}$$

It will be assumed that $|\bar{\theta}|$, $|\bar{\gamma}|$, and k are all $\ll 1$, and all terms of $O(\bar{\theta}^2, \bar{\gamma}^2, \bar{\theta}\bar{\gamma}, \bar{\theta}k^2, \bar{\gamma}k^2)$ and higher will be neglected.

The unit vectors of the coordinate systems introduced above are obviously related by

$$\vec{I} = \vec{i} - \theta\vec{j} \ , \qquad \vec{J} = \theta\vec{i} + \vec{j} \ , \qquad \vec{K} = \vec{k} \tag{6}$$

$$\vec{e}_r = \vec{j}\cos\phi + \vec{k}\sin\phi\,, \qquad \vec{e}_\phi = -\vec{j}\sin\phi + \vec{k}\cos\phi \tag{7}$$

Also, due to the motion of the body we have

$$\frac{d\vec{i}}{dt} = \dot{\theta}\vec{j}\,, \qquad \frac{d\vec{j}}{dt} = -\dot{\theta}\vec{i}\,, \qquad \frac{d\vec{k}}{dt} = 0 \tag{8}$$

Equations (6)-(8) will be used freely throughout the paper. Let the equation of the surface of the body of revolution be given by

$$r = f(x) \tag{9}$$

where, evidently, $f(0) = 0$ in the chosen coordinate system. Then the unit normal vector $\vec{n}$ on the surface is

$$\vec{n} = \mu(x)[\vec{e}_r - \vec{i}f'(x)] \tag{10a}$$

or

$$\vec{n} = \mu(x)[-\vec{i}f'(x) + \vec{j}\cos\phi + \vec{k}\sin\phi] \tag{10b}$$

where

$$\mu(x) = [1 + f'^2(x)]^{-1/2} \tag{11}$$

The position vector of a fluid particle P on the body surface can be written as

$$\vec{\rho} = \vec{i}X + \vec{j}Y + \vec{k}Z \tag{12}$$

where

$$X = x - \theta f(x)\cos\phi \tag{13a}$$

$$Y = Y_c(t) + \theta(x - h) + f(x)\cos\phi \tag{13b}$$

$$Z = f(x)\sin\phi \tag{13c}$$

In order to obtain the Newtonian impact pressure we need to find the normal component of the particle velocity immediately before and after impact. The normal component of velocity before impact is

$$(v_n)_{\text{before}} = \vec{I}\cdot\vec{n} = -\mu(x)[f'(x) + \theta\cos\phi] \tag{14}$$

After impact, a fluid particle moves along the surface and the normal component of its velocity $(v_n)_{after}$ at a point (x,ϕ) is equal to that of the body surface velocity $\vec{v}_b$ itself. Since

$$\vec{v}_b = \left(\frac{d\vec{\rho}}{dt}\right)_{x,\phi \text{ fixed}} = \vec{j}\gamma + \dot{\theta}[-\vec{i}f(x)\cos\phi + \vec{j}(x - h)] \tag{15}$$

we get

$$(v_n)_{after} = \vec{v}_b \cdot \vec{n} = \mu(x)\cos\phi\{\dot{\theta}[x - h + f(x)f'(x)] + \gamma\} \tag{16}$$

Accordingly, the Newtonian impact pressure is

$$p(x,\phi,t)_{impact} = \left[(v_n)_{before} - (v_n)_{after}\right]^2 = \mu^2(x)\{f'^2(x) + 2f'(x)\cos\phi[\theta(t) + \gamma(t)] + 2f'(x)\cos\phi\,\dot{\theta}(t)[x - h + f(x)f'(x)]\} \tag{17}$$

III. Particle Trajectories

As remarked in Ref. 1 (Part I of this study), the Newtonian impact pressure represents the pressure at the outer edge of the Newtonian shock layer, but the pressure at the body surface must contain an additional centrifugal-force correction owing to the curved trajectories followed by the fluid particles subsequent to their impact. In this section we determine the particle trajectories due to the unsteady motion of the body based on the Newtonian assumption that the tangential components of acceleration are zero. We choose two mutually orthogonal unit tangential vectors $\vec{\tau}_1$ and $\vec{\tau}_2$ as follows:

$$\vec{\tau}_1 = \mu(x)[\vec{i} + \vec{e}_r f'(x)] = \mu(x)[\vec{i} + \vec{j}f'(x)\cos\phi + \vec{k}f'(x)\sin\phi] \tag{18a}$$

$$\vec{\tau}_2 = \vec{e}_\phi = -\vec{j}\sin\phi + \vec{k}\cos\phi \tag{18b}$$

The velocity of a particle may be obtained by taking a time derivative of Eq. (12) with the use of Eq. (13). We have

$$\vec{v} = \vec{i}[\dot{x} - \dot{\theta}f(x)\cos\phi] + \vec{j}[\gamma + \dot{\theta}(x - h) + \dot{x}f'(x)\cos\phi - \dot{\phi}f(x)\sin\phi] + \vec{k}[\dot{x}f'(x)\sin\phi + \dot{\phi}f(x)\cos\phi] \tag{19a}$$

or

$$\vec{v} = \vec{\tau}_1\left\{\frac{\dot{x}}{\mu} + \dot{\theta}\mu[(x - h)f' - f]\cos\phi + \gamma\mu f'\cos\phi\right\} + \vec{\tau}_2[-\dot{\theta}(x - h)\sin\phi$$

$$- \gamma\sin\phi + \dot{\phi}f] + \vec{n}[\dot{\theta}\mu(ff' + x - h)\cos\phi + \gamma\mu\cos\phi] \qquad (19b)$$

The velocity $\vec{u}$ of a particle relative to the body may be obtained from Eq. (19b) with $\dot{\theta} = \gamma = 0$. Thus,

$$\vec{u} = \vec{\tau}_1\frac{\dot{x}}{\mu(x)} + \vec{\tau}_2\dot{\phi}f(x) \qquad (20)$$

The acceleration $\vec{a}$ of a particle may then be obtained by taking a time derivative of velocity, yielding

$$\vec{a} = \vec{\tau}_1 a_{\tau_1} + \vec{\tau}_2 a_{\tau_2} + \vec{n}a_n \qquad (21)$$

where

$$a_{\tau_1} = \frac{d}{dt}\left(\frac{\dot{x}}{\mu}\right) - \mu\dot{\phi}^2 ff' + 2\dot{\theta}\mu\dot{\phi}f\sin\phi + \dot{\gamma}\mu f'\cos\phi \qquad (22a)$$

$$a_{\tau_2} = \frac{1}{f}\frac{d}{dt}(f^2\dot{\phi}) - (\dot{\gamma} + 2\dot{\theta}\dot{x})\sin\phi \qquad (22b)$$

$$a_n = \mu\left[\dot{x}^2 f'' - \dot{\phi}^2 f + 2\dot{\theta}\left(\frac{\dot{x}}{\mu^2}\cos\phi - \dot{\phi}ff'\sin\phi\right)\right] + \dot{\gamma}\mu\cos\phi \qquad (22c)$$

The equations governing the motion of the particle are thus

$$\frac{d}{dt}\left(\frac{\dot{x}}{\mu}\right) - \phi^2\mu ff' + 2\dot{\theta}\dot{\phi}\mu f\sin\phi + \dot{\gamma}\mu f'\cos\phi = 0 \qquad (23)$$

$$\frac{d}{dt}(f^2\dot{\phi}) - (\dot{\gamma} + 2\dot{\theta}\dot{x})f\sin\phi = 0 \qquad (24)$$

The initial condition required to determine the particle motion is its velocity immediately after impact. Before impact, a particle's velocity is $\vec{I}$:

$$\vec{I} = \vec{\tau}_1\mu(1 - \theta f'\cos\phi) + \vec{\tau}_2\theta\sin\phi - \vec{n}\mu(f' + 0\cos\phi) \qquad (25)$$

After impact, the particle loses the normal component of its velocity; hence its velocity $\vec{v}_i$ immediately after impact at (x_i, ϕ_i, t_i) is

$$\vec{v}_i = \vec{\tau}_1\mu(x_i)[1 - \theta(t_i)f'(x_i)\cos\phi_i] + \vec{\tau}_2\theta(t_i)\sin\phi_i \qquad (26)$$

Comparing Eq. (26) with the general expression Eq. (19b) for velocity of a particle in the tangent plane, $\vec{v} - \overleftrightarrow{nv} \cdot \vec{n}$, we get the following initial conditions† at $x = x_i$, $\phi = \phi_i$, $t = t_i$:

$$\dot{x} = \mu_i^2\left(1 - \{(\theta + \gamma)f_i' + \dot{\theta}[(x_i - h)f_i' - f_i]\}\cos\phi_i\right) \tag{27a}$$

$$\dot{\phi}f = [(\theta + \gamma) + \dot{\theta}(x_i - h)]\sin\phi_i \tag{27b}$$

In the special case when $\theta = \gamma = 0$, the flow is axisymmetric and we get $\phi = \phi_i$. For small θ and γ, we have

$$\phi = \phi_i + O(\theta,\gamma) \tag{28}$$

We therefore look for solutions to Eqs. (23), (24), and (27) in the form

$$\frac{\dot{x}}{\mu} = A(x) + [\theta E(x) + \dot{\theta}C(x) + \gamma D(x) + \dot{\gamma}E(x)]\cos\phi_i \tag{29a}$$

$$\dot{\phi}f = [\theta F(x) + \dot{\theta}G(x) + \gamma H(x) + \dot{\gamma}K(x)]\sin\phi_i \tag{29b}$$

Substituting Eq. (29) into Eqs. (23), (24), and (27), using the relation

$$\frac{dQ(x)}{dt} = Q'(x)\dot{x} = \mu Q'\{A + [\theta B + \dot{\theta}C + \gamma D + \dot{\gamma}E]\cos\phi_i\} \tag{30}$$

and equating like terms in θ, $\dot{\theta}$, γ, $\dot{\gamma}$, etc., we obtain the following set of ordinary differential equations:

$$AA' = 0\ ; \qquad A(x_i) = \mu_i \tag{31a}$$

$$(AB)' = 0\ ; \qquad B(x_i) = -\mu_i f_i' \tag{31b}$$

$$(AC)' + \frac{B}{\mu} = 0\ ; \qquad C(x_i) = -\mu_i[(x_i - h)f_i' - f_i] \tag{31c}$$

$$(AD)' = 0\ ; \qquad D(x_i) = -\mu_i f_i' \tag{31d}$$

$$(AE)' + \frac{D}{\mu} + f' = 0\ ; \qquad E(x_i) = 0 \tag{31e}$$

---

†Subscript i will denote the value of a function evaluated at $x = x_i$, e.g., $f_i' \equiv \left.\frac{df(x)}{dx}\right|_{x=x_i}$.

$$(fF)' = 0 \; ; \qquad F(x_i) = 1 \tag{31f}$$

$$(fG)' + \frac{fF}{A\mu} - 2f = 0 \; ; \qquad G(x_i) = x_i - h \tag{31g}$$

$$(fH)' = 0 \; ; \qquad H(x_i) = 1 \tag{31h}$$

$$(fK)' + \frac{f(H-1)}{A\mu} = 0 \; ; \qquad K(x_i) = 0 \tag{31i}$$

The solutions to Eqs. (31) are

$$\left.\begin{aligned}
A &= \mu(x_i) \\
B &= D = -\mu(x_i)f'(x_i) \\
C(x,x_i) &= \mu(x_i)[f(x_i) - (x_i - h)f'(x_i)] + f'(x_i)S_o(x,x_i) \\
E(x,x_i) &= -\frac{f(x) - f(x_i)}{\mu(x_i)} + f'(x_i)S_o(x,x_i) \\
F(x,x_i) &= H(x,x_i) = \frac{f(x_i)}{f(x)} \\
G(x,x_i) &= \frac{1}{f(x)}\left[(x_i - h)f(x_i) - \frac{f(x_i)}{\mu(x_i)}S_o(x,x_i) + 2\int_{x_i}^{x} f(\xi)d\xi\right] \\
K(x,x_i) &= \frac{1}{\mu(x_i)f(x)}\int_{x_i}^{x}\frac{f(\xi) - f(x_i)}{\mu(\xi)}\,d\xi
\end{aligned}\right\} \tag{32}$$

where

$$S_n(x,x_i) = \int_{x_i}^{x}\frac{d\xi}{\mu(\xi)f^n(\xi)}, \qquad n = 0,2 \tag{33}$$

IV. Centrifugal Force Correction

As in Ref. 1, the centrifugal pressure is given by

$$p_{centrif} = \int_P^{P'} a_n \rho dn \tag{34}$$

where ρ is density, P is the point on the body surface where pressure is evaluated, and P' is the point at the outer edge of the shock layer across from P. While an expression for a_n, the normal component of acceleration, is readily found from Eq. (22c) plus Eqs. (29) and (32), we need an expression for ρdn. This is obtained from the law of conservation of mass. In a frame of reference fixed with respect to the body, the continuity equation reads

$$\frac{\partial}{\partial t}(\rho dn\, d\phi) + \nabla \cdot (\vec{u}\, \rho dn\, d\phi) = 0 \tag{35}$$

where dn and $d\phi$ are constants fixed with respect to the body and $\vec{u}$ is the particle velocity relative to the body. With

$$\vec{u} = \frac{\dot{x}}{\mu(x)}\vec{\tau}_1 + \vec{\tau}_2 \dot{\phi} f(x) + \vec{n} \cdot 0 \tag{36}$$

and $d\tau_1 = dx/\mu$, $d\tau_2 = f d\phi$, Eq. (35) reduces to

$$\frac{\partial}{\partial t}(\rho dn) + \frac{\mu(x)}{f(x)}\frac{\partial}{\partial x}\left[\frac{f(x)\dot{x}}{\mu(x)}\rho dn\right] + \frac{1}{f(x)}\frac{\partial}{\partial \phi}\left[\dot{\phi} f(x) \rho dn\right] = 0 \tag{37}$$

where the velocity components $\dot{x}/\mu(x)$ and $\dot{\phi} f(x)$ are functions of x, ϕ, and t as given by Eq. (29) (in which ϕ_1 is freely replaced by ϕ) with x_1 appearing as a parameter. Equation (37) is thus a first-order linear partial differential equation for ρdn.

The boundary condition required may be obtained by applying the law of conservation of mass across the shock at the outer edge. Thus, the mass-flow rate of the free stream passing through $d\tau_1 d\tau_2$ at (x_1, ϕ_1) is

$$d\dot{m}_1 = \rho_\infty(\vec{I} - \vec{v}_b) \cdot (-\vec{n}\, d\tau_1 d\tau_2) = f_1[f_1' + (\theta + \gamma)\cos\phi_1 + \dot{\theta}(x_1 - h + f_1 f_1')\cos\phi_1]dx_1\, d\phi_1 \tag{38}$$

whereas the mass-flow rate immediately behind the shock is

$$d\dot{m}_2 = \rho(x_i,\phi_i)|\vec{u}|f_i\, dn\, d\phi_i = \left[\frac{\dot{x}}{\mu} f\, \rho dn\right]_{x=x_i} d\phi_i \tag{39}$$

Conservation of mass demands $d\dot{m}_1 = d\dot{m}_2$ and this yields the required boundary condition that at $x = x_i$, $\phi = \phi_i$, $t = t_i$:

$$\frac{\dot{x}}{\mu}\rho dn = [f_i' + (\theta + \gamma)\cos\phi_i + \dot{\theta}(x_i - h + f_i f_i')\cos\phi_i]dx_i \tag{40}$$

The solution to Eq. (37) with boundary condition Eq. (40) is sought in the form

$$\rho dn = \frac{1}{f(x)}\{\hat{A}(x) + [\theta\hat{B}(x) + \dot{\theta}\hat{C}(x) + \gamma\hat{D}(x) + \dot{\gamma}\hat{E}(x)]\cos\phi\}dx_i \tag{41}$$

Substituting Eq. (41) into Eqs. (37) through (40), and equating like terms in θ, $\dot{\theta}$, γ, $\dot{\gamma}$, etc., we obtain the following set of ordinary differential equations for the determination of $\hat{A}$ to $\hat{E}$:

$$(A\hat{A})' = 0\ ; \qquad (A\hat{A})_i = f_i f_i' \tag{42a}$$

$$(B\hat{A} + A\hat{B})' + \frac{\hat{A}F}{\mu f} = 0\ ; \qquad (B\hat{A} + A\hat{B})_i = f_i \tag{42b}$$

$$(C\hat{A} + A\hat{C})' + \frac{\hat{A}G}{\mu f} + \frac{\hat{B}}{\mu} = 0\ ; \qquad (C\hat{A} + A\hat{C})_i = f_i[x_i - h + f_i f_i'] \tag{42c}$$

$$(D\hat{A} + A\hat{D})' + \frac{\hat{A}H}{\mu f} = 0\ ; \qquad (D\hat{A} + A\hat{D})_i = f_i \tag{42d}$$

$$(E\hat{A} + A\hat{E})' + \frac{\hat{A}K}{\mu f} + \frac{\hat{D}}{\mu} = 0\ ; \qquad (E\hat{A} + A\hat{E})_i = 0 \tag{42e}$$

Equations (42) can be solved successively, yielding

$$\hat{A} = \frac{f(x_i)f'(x_i)}{\mu(x_i)} \tag{43a}$$

$$\hat{B}(x,x_i) = \hat{D}(x,x_i) = \frac{f(x_i)}{\mu^3(x_i)}[1 - \mu(x_i)t(x_i)f'(x_i)S_2(x,x_i)] \tag{43b}$$

$$\hat{C}(x,x_1) = \frac{f(x_1)}{\mu(x_1)}\left\{\frac{x_1 - h}{\mu^2(x_1)} - \frac{(x_1 - h)}{\mu(x_1)} f(x_1)f'(x_1)S_2(x,x_1)\right.$$

$$- \frac{2f'(x_1)}{\mu(x_1)} \int_{x_1}^{x} \frac{d\xi}{\mu(\xi)f^2(\xi)} \int_{x_1}^{\xi} f(s)ds - \frac{[1 + f'^2(x_1)\mu^2(x_1)]}{\mu^3(x_1)} S_0(x,x_1)$$

$$\left. + \frac{f(x_1)f'(x_1)}{\mu^2(x_1)} S_0(x,x_1)S_2(x,x_1)\right\} \tag{43c}$$

$$\hat{E}(x,x_1) = \frac{f(x_1)}{\mu(x_1)}\left\{\frac{f'(x_1)}{\mu^2(x_1)}[f(x) - f(x_1)] - \frac{[1 + f'^2(x_1)\mu^2(x_1)]}{\mu^3(x_1)} S_0(x,x_1)\right.$$

$$\left. + \frac{f(x_1)f'(x_1)}{\mu^2(x_1)} S_0(x,x_1)S_2(x,x_1) - \frac{f'(x_1)}{\mu^2(x_1)} \int_{x_1}^{x} \frac{d\xi}{\mu(\xi)f^2(\xi)} \int_{x_1}^{\xi} \frac{f(s)}{\mu(s)} ds\right\} \tag{43d}$$

We are now in a position to calculate the centrifugal pressure correction. The normal component of acceleration is, from Eqs. (22c), (29), and (32),

$$a_n(x,\phi,t;x_1) = \kappa(x)A^2 + 2\left\{\theta\kappa(x)AB + \dot{\theta}[\kappa(x)AC + A]\right.$$

$$\left. + \gamma\kappa(x)AD + \dot{\gamma}\left[\kappa(x)AE + \frac{\mu(x)}{2}\right]\right\} \cos\phi \tag{44}$$

where

$$\kappa(x) = \mu^3(x)f''(x) \tag{45}$$

is the curvature of the body surface along direction $\vec{\tau}_1$ (the curvature of the body surface along direction $\vec{\tau}_2$ is, of course, equal to $-1/f(x)$ for the body of revolution). Putting Eqs. (41) and (44) into Eq. (34), using the solution Eq. (43), and expanding and neglecting terms of $O(\bar{\theta}^2, \bar{\gamma}^2, \bar{\theta}\bar{\gamma})$, we get the centrifugal pressure correction:

$$p_{centrif}(x,\phi,t)$$

$$= \frac{\kappa(x)}{f(x)} \int_0^x \mu(\xi)f(\xi)f'(\xi)d\xi + (\theta + \gamma)\cos\phi \frac{\kappa(x)}{f(x)} \int_0^x \{\mu(\xi)f(\xi)[1 - f'^2(\xi)]$$

$$- f^2(\xi)f'(\xi)S_2(x,\xi)\}d\xi + \dot{\theta}\cos\phi \frac{\kappa(x)}{f(x)} \int_0^x [\mu^2(\xi)\hat{C}(x,\xi)$$

$$+ 2f(\xi)f'(\xi)C(x,\xi)]d\xi + \dot{\theta}\cos\phi\, f(x) + \dot{\gamma}\cos\phi \frac{\kappa(x)}{f(x)} \int_0^x [\mu^2(\xi)\hat{E}(x,\xi)$$

$$+ 2f(\xi)f'(\xi)E(x,\xi)]d\xi + \dot{\gamma}\cos\phi \frac{\mu(x)}{f(x)} \int_0^x \frac{f(\xi)f'(\xi)}{\mu(\xi)}\, d\xi \qquad (46)$$

Adding Eq. (46) to Eq. (17), we get for the surface pressure

$$p(x,\phi,t) = P_0(x) + \cos\phi\{[\theta(t) + \gamma(t)]P_1(x)$$

$$+ \dot{\theta}(t)[P_2(x) - hP_1(x)] + \dot{\gamma}(t)P_3(x)\} \qquad (47)$$

where

$$P_0(x) = \mu^2(x)f'^2(x) + \frac{\kappa(x)}{f(x)} \int_0^x \mu(\xi)f(\xi)f'(\xi)d\xi \qquad (48a)$$

$$P_1(x) = 2\mu^2(x)f'(x) + \frac{\kappa(x)}{f(x)} \int_0^x \{\mu(\xi)f(\xi)[1 - f'^2(\xi)] - f^2(\xi)f'(\xi)S_2(x,\xi)\}d\xi \qquad (48b)$$

$$P_2(x) = 2\mu^2(x)f'(x)[x + f(x)f'(x)] + f(x) + \frac{\kappa(x)}{f(x)} \int_0^x \Bigg\{\xi f(\xi)\mu(\xi)[1 - f'^2(\xi)]$$

$$+ 2\mu(\xi)f^2(\xi)f'(\xi) - f(\xi)S_0(x,\xi) + \frac{f^2(\xi)f'(\xi)}{\mu(\xi)} S_0(x,\xi)S_2(x,\xi)$$

$$- \xi f^2(\xi)f'(\xi)S_2(x,\xi) - 2f(\xi)f'(\xi)\int_\xi^x \frac{d\eta}{\mu(\eta)f^2(\eta)} \int_\xi^\eta f(\zeta)d\zeta\Bigg\}d\xi \qquad (48c)$$

$$P_3(x) = \frac{\mu(x)}{f(x)} \int_0^x \frac{f(\xi)f'(\xi)d\xi}{\mu(\xi)} + \frac{\kappa(x)}{f(x)} \int_0^x [\mu^2(\xi)\hat{E}(x,\xi) + 2f(\xi)f'(\xi)E(x,\xi)]d\xi \qquad (48d)$$

The expressions in Eqs. (48) may be further simplified by elementary operations on the integral terms, yielding

$$P_1(x) = 2\mu^2(x)f'(x) + \frac{2}{3}\frac{\kappa(x)}{f(x)} \int_0^x \mu(\xi)f(\xi)[1 - 2f'^2(\xi)]d\xi \qquad (49a)$$

$$P_2(x) = \mu^2(x)[f(x) + 2xf'(x) + 3f(x)f'^2(x)]$$

$$+ \frac{\kappa(x)}{f(x)} [J_1(x) - J_2(x) - J_3(x) + J_4(x)] \qquad (49b)$$

$$P_3(x) = \frac{\mu(x)}{f(x)} J_5(x) + \frac{\kappa(x)}{f(x)} \left\{ -J_2(x) + J_4(x) - \int_0^x J_5'(\xi)[f(x) - f(\xi)]d\xi \right.$$
$$\left. - \int_0^x \frac{f(\xi)}{\mu(\xi)} J_5(\xi) S_2(x,\xi) d\xi \right\} \tag{49c}$$

where

$$\left.\begin{aligned}
J_1(x) &= \frac{2}{3} \int_0^x \mu(\xi) f(\xi) \{\xi[1 - 2f'^2(\xi)] \\
&\quad + 3f(\xi)f'(\xi)\} d\xi \\
J_2(x) &= \int_0^x f(\xi) S_0(x,\xi) d\xi \\
J_3(x) &= \frac{2}{3} \int_0^x f^3(\xi) S_2(x,\xi) d\xi \\
J_4(x) &= \int_0^x \frac{f^2(\xi) f'(\xi)}{\mu(\xi)} S_0(x,\xi) S_2(x,\xi) d\xi \\
J_5(x) &= \int_0^x \frac{f(\xi) f'(\xi)}{\mu(\xi)} d\xi
\end{aligned}\right\} \tag{50}$$

In summary, with the shape function $f(x)$ of a body of revolution given, the Newton-Busemann surface pressure in unsteady flow can be obtained by quadrature. The function $P_1(x)$ in Eq. (49a), which represents the perturbation pressure at small incidence in steady flow, is identical with that given by Hayes and Probstein[2] (when a misprint in Ref. 2 is corrected: the upper limit of the integral (3.8.17) of Ref. 2 should be x_1 instead of 1). The functions $P_2(x)$ and $P_3(x)$ are new, giving the out-of-phase pressure components arising from unsteady motions in 0 and γ, respectively.

V. Stability of Oscillating Bodies of Revolution

The general results for unsteady surface pressure obtained in Sec. IV will now be used to study the dynamic stability of bodies of revolution. As in Ref. 1, the principal motion variables are taken to be the angle of pitch $\theta(t)$ and the angle of attack $\alpha(t)$, where $\alpha(t) = \theta(t) + \gamma(t)$. Equation (47) is then recast as

$$p(x,\phi,t) = P_0(x) + \cos\phi\{\alpha(t)P_1(x) + \dot{\theta}(t)[P_2(x) - P_3(x) - hP_1(x)] + \dot{\alpha}(t)P_3(x)\} \tag{51}$$

The normal force and pitching-moment coefficients are again defined as usual

$$C_N = \frac{N}{(1/2)\rho_\infty U_\infty^2 S_b}, \quad C_m = \frac{M}{(1/2)\rho_\infty U_\infty^2 S_b \ell} \tag{52}$$

where S_b is the base area of the body, N is the normal force, and M is the moment of surface-pressure force about the pivot axis C. The various stability derivatives are defined as in Ref. 1. Thus,

$$C_{N_\psi} = \frac{2}{\pi f^2(1)} \iint_S \frac{\partial}{\partial\psi} p(x,\phi,t)\cos\phi \, dS, \quad \psi = \dot{\theta},\alpha,\dot{\alpha}$$

$$-C_{m_\psi} = \frac{2}{\pi f^2(1)} \iint_S \frac{\partial}{\partial\psi} p(x,\phi,t)[x - h + f(x)f'(x)]\cos\phi \, dS, \quad \psi = \dot{\theta},\alpha,\dot{\alpha} \tag{53}$$

where S is the lateral surface of the body of revolution. The stability derivatives introduced above are also related through the axis-transfer rules given by Eq. (59) of Ref. 1. In this paper we shall study in detail the stability of the pitching motion of classes of bodies of revolution in rectilinear flight [$\gamma(t) = 0$, $\theta(t) = \alpha(t)$]. In this case the stiffness derivative $-C_{m_\theta}$ and the damping-in-pitch derivative $-C_{m_{\dot{\theta}}}$ take the form

$$-C_{m_\theta} = \frac{2}{f^2(1)} \int_0^1 P_1(x)f(x)[x - h + f(x)f'(x)]dx \tag{54a}$$

$$-C_{m_{\dot{\theta}}} = \frac{2}{f^2(1)} \int_0^1 [P_2(x) - hP_1(x)]f(x)[x - h + f(x)f'(x)]dx \tag{54b}$$

Circular Cones

For a cone

$$f(x) = x \tan \tau \tag{55}$$

where the constant τ is the semivertex angle of the cone. From Eq. (49), we get

$$P_0 = \sin^2 \tau \ , \ P_1 = 2 \sin \tau \cos \tau \ , \ P_2 = 3x \tan \tau \tag{56}$$

whence from Eq. (54)

$$-C_{m_\theta} = 2\left(\frac{2}{3} - h \cos^2 \tau\right) \equiv F(h) \tag{57a}$$

$$-C_{m_{\dot\theta}} = \frac{2}{\cos^2 \tau}\left[\frac{3}{4} - \frac{5}{3} h \cos^2 \tau + (h \cos^2 \tau)^2\right] \equiv \frac{G(h)}{\cos^2 \tau} \tag{57b}$$

The stiffness derivative formula (Eq. (57a)) according to Newtonian theory has been extensively demonstrated (cf. Figs. 8-11 of Ref. 3) to yield very good agreement with the results of experiments for a 10° cone in air flows at Mach numbers greater than 5. Equation (57b) for the damping-in-pitch derivative of a cone is, on the other hand, new and heretofore unverified. It contains the centrifugal force correction due to the curved paths followed by fluid particles in unsteady motion and generalizes the result of Mahood and Hui[4] to include the dependence on pivot position h.

Although, for a cone, a centrifugal force correction is not required for steady flow, such a correction <u>is</u> required for unsteady flow and, in fact, is fully as important as the impact pressure contribution. This is clearly demonstrated in Fig. 2, in which the full damping-in-pitch coefficient with centrifugal force correction included (Eq. (57b)) is compared with the coefficient that results from consideration of the impact pressure alone, namely (from Eq. (17)),

$$\left(-C_{m_{\dot{\theta}}}\right)_{\text{impact}} = \frac{2}{\cos^2 \tau}\left[\frac{1}{2} - \frac{4}{3} h \cos^2 \tau + (h \cos^2 \tau)^2\right] \tag{58}$$

The difference between the two results in Fig. 2 is a direct measure of the centrifugal force contribution, which, analytically, takes the form

$$\left(-C_{m_{\dot{\theta}}}\right)_{\text{centrif}} = \frac{2}{\cos^2 \tau}\left[\frac{1}{4} - \frac{1}{3} h \cos^2 \tau\right] \tag{59}$$

It will be seen in Fig. 2 that the centrifugal-force contribution (Eq. (59)) can be of the same order of magnitude as the impact pressure contribution (Eq. (58)). This result casts doubt on the validity of various unsteady Newtonian flow theories that are based on the Newtonian impact pressure alone. For example, Ericsson's theory,[7] in which $-C_{m_q}$ is calculated from the Newtonian impact pressure alone and then added to an estimate of $-C_{m_{\dot{\alpha}}}$ to give the equivalent $-C_{m_{\dot{\theta}}}$, must be incorrect in at least the separate components, if not the sum, since both components contain centrifugal-force contributions. These separate contributions can be deduced from the results presented in Eq. (49). Thus, the centrifugal-force component in $-C_{m_{\dot{\alpha}}}$ (which, for this coefficient, is also the total since there is no impact pressure component) is calculated from $P_3(x)$ alone, and takes the form

$$\left(-C_{m_{\dot{\alpha}}}\right)_{\text{centrif}} = \frac{1}{\cos^2 \tau}\left[\frac{1}{4} - \frac{1}{3} h \cos^2 \tau\right] \tag{60}$$

which is seen to be exactly one half of the total centrifugal-force component in $-C_{m_{\dot{\theta}}}$ (Eq. (59)). It may be easily verified that the centrifugal-force component in $-C_{m_q}$ contributes the other half. This result, which is also true for the wedge airfoil (cf. Eq. (51) of Ref. 1) may be summarized as follows: the centrifugal force components in $-C_{m_q}$ and $-C_{m_{\dot{\alpha}}}$ are equal (for cones and wedge airfoils), and therefore each coefficient contributes exactly one half of the centrifugal-force component in $-C_{m_{\dot{\theta}}}$.

There is yet another aspect of this result that warrants consideration. The fact that $-C_{m_q}$ has a significant centrifugal-force component means that even in the Newtonian limit, an accurate estimate of $-C_{m_q}$ cannot be derived on the basis of a local analysis, such as impact theory, or in fact any theory in which local pressure is said to depend solely on the local flow velocity. On the contrary, the presence of a centrifugal-force term is an indication of the influence of flow history on the local pressure. Since a local analysis for $-C_{m_q}$ is inadequate even in the Newtonian limit, this should give pause to those proposing to predict aerodynamic stability derivatives at lower speeds on the basis of similar local analyses.

Also plotted in Fig. 2 are the results of measurements for the damping-in-pitch coefficient carried out in air flow at a free-stream Mach number of 10 by Hobbs[5] and the results of numerical computations based on an inviscid gas-dynamic theory carried out by Brong.[6] It will be seen that results based on the complete Newton-Busemann theory are in excellent agreement with the experimental results for the highest Reynolds number presented; the numerical results of Brong agree better with the experimental results for lower Reynolds numbers. We believe that it is partly fortuitous, and not an indication of the superiority of Newton-Busemann theory, that results from the latter theory should be in closer agreement with the experimental results at the highest Reynolds number than those of the gas-dynamic theory. In Ref. 8, dealing with gas-dynamic theory, it has been shown that both increasing the free-stream Mach number M_∞ and decreasing the ratio of specific heats γ tend to increase the damping-in-pitch coefficient $-C_{m_{\dot{\theta}}}$. Consequently, Newton-Busemann theory, the theory that results from taking the double limit $M_\infty \to \infty$, $\gamma \to 1$ of gas-dynamic theory, should overestimate $-C_{m_{\dot{\theta}}}$ for finite values of M_∞ and for values of γ greater than unity ($\gamma = 1.4$ for air). Physically, this is

because in the Newtonian limit the shock layer becomes infinitesimally thin, thus eliminating one mechanism of dynamic destabilization, namely, the phase lag resulting from pressure signals traveling to and reflecting from the bow shock. Since Newton-Busemann theory should have overpredicted $-C_{m_{\dot{\theta}}}$, the close agreement evidenced in Fig. 2 between results from Newton-Busemann theory and the experimental results at the highest Reynolds number must be attributed to the presence of the boundary layer on the body in the experiments, which, in the usual way, may be considered to have formed an effective displacement surface. The effective thickness of the cone would have increased thereby, providing a mechanism for a corresponding increase in $-C_{m_{\dot{\theta}}}$. Thus, the Newton-Busemann theory may have overpredicted $-C_{m_{\dot{\theta}}}$ by just the right amount to account for viscous effects.

Finally, we note in Eq. (57b) that analogous to the wedge airfoil (Eq. (62)), Ref. 1), the damping-in-pitch coefficient $-C_{m_{\dot{\theta}}}$ for a cone is always positive according to Newton-Busemann theory. Hence, the pitching motion of a cone of any thickness and about any axis position is dynamically stable in the Newtonian limit.

Blunt Cones

To investigate the effects of nose bluntness on the dynamic stability, we consider a class of bodies in which, for each body, the nose consists of a spherical cap, and the afterbody is the frustum of a circular cone which joins the spherical cap smoothly and with a common tangent (Fig. 3). Let the radius of the spherical cap be R_N and the radius of the base of the cone be R_B. Then the class of bodies under consideration is described by the following parameters: the semiangle of the cone τ, the ratio $\lambda = R_N/R_B$, and the (actual) length of the body (from nose to base) $\ell = 1$. Let $s = (1 - \sin\tau)/\sin\tau$; then

$$R_N = \frac{\lambda \tan \tau}{1 - s\lambda \tan \tau}$$

Let $j = sR_N$; then the length c of the full cone is $c = 1 + j$ and $R_B = (1 + j)\tan \tau$. The equation of the body is given by

$$r = f(x) = \begin{cases} (2R_N x - x^2)^{1/2} ; & 0 \le x \le j \sin \tau \\ (x + j)\tan \tau ; & j \sin \tau \le x \le 1 \end{cases} \tag{61}$$

Each of the stability derivatives consists of two parts, the first deriving from the pressure on the spherical surface $(\ )_s$, and the second from the pressure on the conical surface $(\ )_c$. Thus,

$$\left.\begin{aligned} \left(-C_{m_\theta}\right) &= \left(-C_{m_\theta}\right)_s + \left(-C_{m_\theta}\right)_c \\ \left(-C_{m_{\dot\theta}}\right) &= \left(-C_{m_{\dot\theta}}\right)_s + \left(-C_{m_{\dot\theta}}\right)_c \end{aligned}\right\} \tag{62}$$

On the spherical surface, using Eq. (61a), we get from Eq. (49a),

$$P_1(x) = \frac{8}{3}(1 - x_1)(2x_1 - x_1^2)^{1/2}, \qquad \left(0 \le x_1 \equiv \frac{x}{R_N} \le 1 - \sin \tau\right) \tag{63}$$

It can also be shown, either by physical reasoning based on Eq. (47) or by direct computation in Eq. (48), that

$$P_2(x) = R_N P_1(x) \tag{64}$$

Reasoning physically, we note in Eq. (47) that the contribution due to the nose cap to the pressure component proportional to $\dot\theta$ must be zero when the axis h, about which the body turns, passes through the center of the spherical nose cap (i.e., $h = R_N$), for then the curve defining the nose-cap surface turns on itself and there is no change in the body geometry, so far as the inviscid external flow is concerned, to alert it that the nose cap is turning. We see from Eq. (47) that the pressure component proportional to $\dot\theta$ will be zero at $h = R_N$ if and only if Eq. (64) is true. Using Eqs. (63) and (64) to evaluate the contribution of the nose cap to $-C_{m_\theta}$ and $-C_{m_{\dot\theta}}$, we get

$$\left.\begin{aligned}\left(-C_{m_\theta}\right)_s &= \frac{4}{3}\lambda^2\cos^4\tau(R_N - h)\\ \left(-C_{m_{\dot\theta}}\right)_s &= \frac{4}{3}\lambda^2\cos^4\tau(R_N - h)^2\end{aligned}\right\} \tag{65}$$

On the conical afterbody, $\kappa(x) = 0$, hence $P_1(x) = 2\sin\tau\cos\tau$ and $P_2(x) = [3x + j(1 + 2\sin^2\tau)]\tan\tau$. These show that, owing to the vanishing of κ, the pressures on the conical afterbody depend on the local position x, but not on the body shape upstream of x.[5] Making use of this property in calculating the contributions to $-C_{m_\theta}$ and $-C_{m_{\dot\theta}}$ due to the conical afterbody, we are permitted to build up the contributions of the afterbody out of the contributions from full cones; that is, those of a large cone with origin at the apex of the conical frustum and base at the base of the frustum (cf. Fig. 3), less those of a small cone with origin at the same apex and base at the foot of the frustum. We get

$$\left.\begin{aligned}\left(-C_{m_\theta}\right)_c &= (1 + j)\left[F(x_o) - \beta^3 F\left(\frac{x_o}{\beta}\right)\right]\\ \left(-C_{m_{\dot\theta}}\right)_c &= \frac{(1 + j)^2}{\cos^2\tau}\left[G(x_o) - \beta^4 G\left(\frac{x_o}{\beta}\right)\right]\end{aligned}\right\} \tag{66}$$

where $\beta = \lambda\cos\tau$ and $x_o = (h + j)/(1 + j)$ is the pivot position from the apex of the large cone relative to its length c (Fig. 3). The functions F and G are defined in Eqs. (57). It should be apparent that each of the first terms in Eqs. (66) represents the contribution of the large cone, and that each of the second terms represents the (subtractive) contribution of the small cone.

---

[5] This property, which holds for conical bodies only in the Newtonian limit, makes the theory a local one in the sense that the pressure at a point x is "unaware" that the frustum is not a full cone.

In the greater part of the literature dealing with the stability of blunt cones,[7,9] the pitching-moment coefficient and the stability derivatives are defined with the length c of the extended sharp cone being used as the characteristic length rather than the actual body length that is used in this paper. We note here that the stiffness and damping-in-pitch coefficients from Refs. 7 and 9, formed with c as characteristic length, are equal to $-(1 + j)^{-1}C_{m_\theta}$, $-(1 + j)^{-2}C_{m_{\dot\theta}}$, respectively, in our notation. The effects of bluntness on the stability derivatives may be examined by forming the ratios of the derivatives with their counterparts for sharp cones. Combining Eqs. (65) and (66), we get

$$\left.\begin{aligned}
\frac{(1 + j)^{-1}C_{m_\theta}}{\left[(1 + j)^{-1}C_{m_\theta}\right]_{R_N=0}} &= 1 + \frac{\beta^2}{F(x_o)}\left[-\beta F\left(\frac{x_o}{\beta}\right) + \frac{4}{3}(\beta - x_o\cos^2\tau)\right] \\
\frac{(1 + j)^{-2}C_{m_{\dot\theta}}}{\left[(1 + j)^{-2}C_{m_{\dot\theta}}\right]_{R_N=0}} &= 1 + \frac{\beta^2}{G(x_o)}\left[-\beta^2 G\left(\frac{x_o}{\beta}\right) + \frac{4}{3}(\beta - x_o\cos^2\tau)^2\right]
\end{aligned}\right\} \quad (67)$$

For small bluntness, $\lambda = R_N/R_B \ll 1$, hence $\beta \ll 1$, and the right-hand sides of Eqs. (67) both reduce to $1 + 0(\lambda^2)$, showing that the effect of nose bluntness should be negligibly small for small bluntness. This theoretical prediction is borne out by a comparison of experimental results with computations based on Newton-Busemann theory for blunted cones (with τ fixed at 10° and x_o fixed at 0.6). The comparisons are presented in Figs. 4 and 5, where the experimental points have been taken from an extensive compilation provided by Khalid and East in Ref. 9. We note in Fig. 4 that the experimental results for C_{m_θ} would appear to confirm the initial behavior predicted by Newton-Busemann theory for values of λ up to about 0.07. Similarly, in Fig. 5, as predicted by Newton-Busemann theory, experimental results for $C_{m_{\dot\theta}}$ initially do not vary

significantly with λ for values of the parameter up to about 0.05. As the bluntness parameter increases, however, Newton-Busemann theory is incapable of predicting the abrupt and large variation with bluntness that is observed experimentally in air flow with $\gamma = 1.4$ for both the stiffness and the damping-in-pitch coefficients. This incapacity is symptomatic of Newtonian flow theory, both steady and unsteady, in cases where a principal requirement of the theory is violated, namely, that the shock layer remain everywhere thin. As seen in Fig. 6 for spherically blunted cones, as the nose bluntness increases, the shock overexpands around the nose cap, creating a shock layer of significant thickness on the conical afterbody. Possible amendments to the theory are discussed in Sec. VI. It is of interest to note that computations based on a complete gas-dynamic theory[10] — results from which are also plotted on Figs. 4 and 5 — suggest that gas-dynamic theory is capable of capturing the major features of the dependence on bluntness. Curiously, however, as computed, the numerical results miss the initial behavior of the derivatives as a function of bluntness parameter.

Slender Power-Law Bodies

For slender bodies, $f(x) = O(b)$ with $b \ll 1$. When terms of $O(b^3)$ are neglected compared with terms retained of $O(b)$, the formulas for surface pressure (cf. Eqs. (49) and (50)) simplify to

$$\left.\begin{aligned} P_0(x) &= f'^2(x) + \frac{1}{2} f(x)f''(x) \\ P_1(x) &= 2f'(x) + \frac{2}{3}\frac{f''(x)}{f(x)} \int_0^x f(\xi)d\xi \\ P_2(x) &= f(x) + 2xf'(x) + \frac{1}{3}\frac{f''(x)}{f(x)} \int_0^x [2\xi f(\xi) \\ &\quad - 2\int_0^\xi f(\eta)d\eta - \frac{1}{f^2(\xi)} \int_0^\xi f^3(\eta)d\eta]d\xi \end{aligned}\right\} \tag{68}$$

For power-law bodies of revolution

$$f(x) = bx^n \tag{69}$$

we get

$$\left.\begin{aligned} P_0(x) &= b^2 \frac{n(3n-1)}{2} x^{2n-2} \\ P_1(x) &= bM_1 x^{n-1} \\ P_2(x) &= bM_2 x^n \end{aligned}\right\} \tag{70}$$

where

$$\begin{aligned} M_1 &= \frac{4}{3}\frac{n(2n+1)}{n+1} \\ M_2 &= (2n+1)\left[1 + \frac{n(n-1)(3n-1)}{3(n+1)(n+2)(3n+1)}\right] \end{aligned} \tag{71}$$

The damping-in-pitch derivative is

$$-C_{m_{\dot\theta}} = \frac{M_2}{n+1} - 2\frac{M_1+M_2}{2n+1}h + \frac{M_1}{n}h^2 \tag{72}$$

For Newton-Busemann flow theory to apply, it is required that $P_0(x) \geq 0$, hence $n \geq 1/3$. The damping-in-pitch derivative Eq. (72) has a minimum value given by

$$\left(-C_{m_{\dot\theta}}\right)_{min} = \frac{3}{n(2n+1)}\left[M_1M_2 - n(n+1)\left(\frac{M_1+M_2}{2n+1}\right)^2\right] \tag{73}$$

which is plotted in Fig. 7 as a function of the power n. It is seen that increasing the power n, that is, making the shape of the body more concave, tends to decrease $(-C_{m_{\dot\theta}})_{min}$. In this sense it may be said that increasing the convexity of slender power-law bodies of revolution has a favorable effect on the dynamic stability of the bodies. This conclusion is similar to that reached in Ref. 1 for slender power-law airfoils. However, for bodies of revolution, $(-C_{m_{\dot\theta}})_{min} > 0$ for all n, implying that the pitching motions of slender power-law bodies of revolution are always dynamically stable. In contrast,

slender power-law airfoils of concave shape may be dynamically unstable if the surface curvature exceeds a certain limit.

VI. Concluding Remarks

In this paper, we have developed a complete unsteady Newton-Busemann flow theory for oscillating bodies of revolution of arbitrary shape having sharp or blunt noses. Exact formulas in closed form are given for the stability derivatives of these bodies; they require only numerical quadratures of terms involving the body shape.

The centrifugal force arising from the curved trajectories followed by the fluid particles in unsteady flow is shown to be very important. Its contribution cannot be neglected, even for a circular cone for which the centrifugal force contribution is zero in steady flow. With this correction included, the theory is shown to be in excellent agreement with experimental results for sharp cones and for cones with small nose bluntness.

However, as expected from the incapability of steady Newton-Busemann flow theory to predict the surface pressure on blunt-nosed bodies in air flow (with $\gamma = 1.4$), the unsteady Newton-Busemann flow theory also gives poor results for stability derivatives of bodies with moderate or large nose bluntness. This is primarily due to the violation of the principal requirement of the theory in such flow, namely, that the shock layer remain everywhere infinitesimally thin. Improvements may result by using the thin-shock-layer theory, in which solutions to the full gas-dynamic equations are sought in the form of a power series in the thickness of the shock layer. The unsteady Newton-Busemann flow given here would then provide the leading term in such a rational expansion scheme. For configurations such that the shock layer remains everywhere thin, the thin-shock-layer theory may be expected to give only small corrections to the Newton-Busemann theory. Such is the situation in the case of an oscillating delta wing.

Indeed, it can be shown[11] that the thin-shock-layer theory for oscillating delta wings[12] gives results almost identical with those obtained with unsteady Newton-Busemann theory.

An alternative but empirical approach, which may produce improvement in predictive power over the present theory, would be to apply the concept of embedded Newtonian flow.[7,13] The application is made feasible by the availability now of a complete description of the unsteady flow field based on the Newton-Busemann concept.

Acknowledgment

We thank M. F. Platzer for many useful discussions during the course of research leading to this paper.

References

[1]Hui, W. H. and Tobak, M., "Unsteady Newton-Busemann Flow Theory, Part I: Airfoils," submitted to AIAA Journal.

[2]Hayes, W. D. and Probstein, R. F., Hypersonic Flow Theory, 2nd ed., Vol. 1, Academic Press, 1966, pp. 201-204.

[3]Welsh, C. J., Winchenbach, G. L., and Madagan, A. N., "Free-Flight Investigation of the Aerodynamic Characteristics of a Cone at High Mach Numbers," AIAA Journal, Vol. 8, No. 2, 1970, pp. 294-300.

[4]Mahood, G. E. and Hui, W. H., "Remarks on Unsteady Newtonian Flow Theory," Aeronautical Quarterly, Vol. 27, 1976, pp. 35-44.

[5]Hobbs, R. B., "Results of Experimental Studies on the Hypersonic Dynamic Stability Characteristics of a 10° Cone at M = 20°," General Electric ATDM 1:37, May 1964.

[6]Brong, E. A., "The Flow Field About a Right Circular Cone in Unsteady Flight," AIAA Paper 65-398, 1965.

[7]Ericsson, L. E., "Unsteady Embedded Newtonian Flow," Astronautics Acta, Vol. 18, 1973, pp. 309-330.

[8]Hui, W. H., "An Analytical Theory of Supersonic/Hypersonic Stability at High Angles of Attack," AGARD Conference Proceedings CP-235, 1978.

[9]Khalid, M. and East, R. A., "Stability Derivatives of Blunt Slender Cones at High Mach Numbers," Aeronautical Quarterly, Vol. 30, 1979, pp. 559-599.

[10]Rie, T., Linkiewicz, E. A., and Bosworth, F. D., "Hypersonic Dynamic Stability, Part III, Unsteady Flow Field Program," FDL-TDR-64-149, Jan. 1967, Air Force Flight Dynamics Lab., Wright-Patterson Air Force Base.

[11]Hui, W. H. and Platzer, M. F., "Stability of Oscillating Supersonic/Hypersonic Wings at Arbitrary Angles of Attack" (to be published).

[12]Hui, W. H. and Hemdan, H. T., "Unsteady Hypersonic Flow Over Delta Wings with Detached Shock Waves," AIAA Journal, Vol. 14, No. 4, 1976, pp. 505-511.

[13]Seiff, A., "Secondary Flow-Fields Embedded in Hypersonic Shock Layers," NASA TN D-1304, 1962.

FIGURE CAPTIONS

Fig. 1 Oscillating body of revolution.

Fig. 2 Comparison of theory and experiment for damping-in-pitch derivative of a 10° sharp cone.

Fig. 3 Geometry of blunt cone.

Fig. 4 Variation of 10° cone stiffness derivative with bluntness – comparison of theory and experiment.

Fig. 5 Variation of damping-in-pitch derivative with nose bluntness – comparison of theory and experiment.

Fig. 6 Variation of shock-layer thickness with bluntness of a 12.5° cone in hypersonic air flow. (Courtesy of G. Malcolm, NASA, Ames Research Center.)

Fig. 7 Variation with power n of minimum damping-in-pitch derivative for slender power-law body.

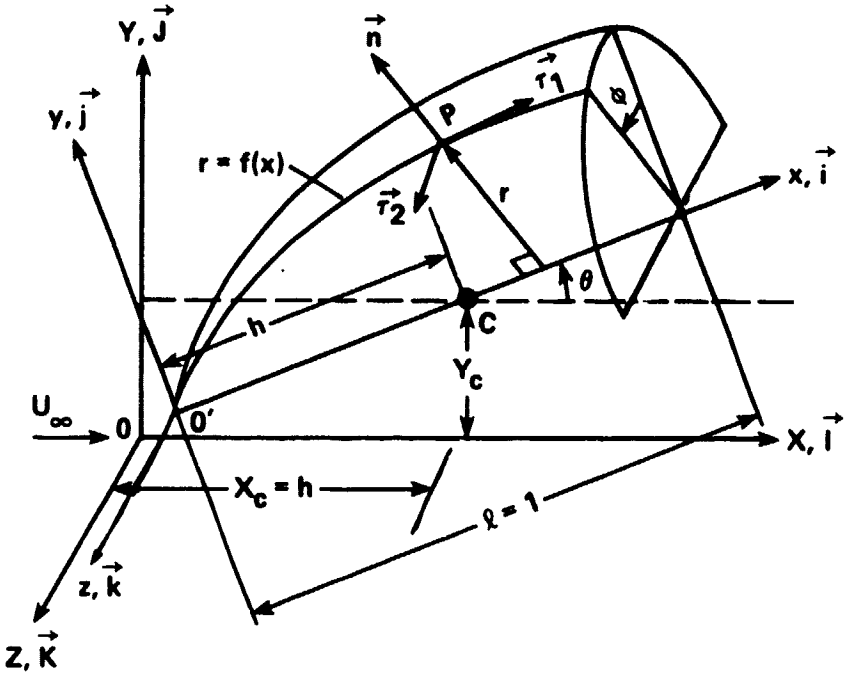

Fig. 1

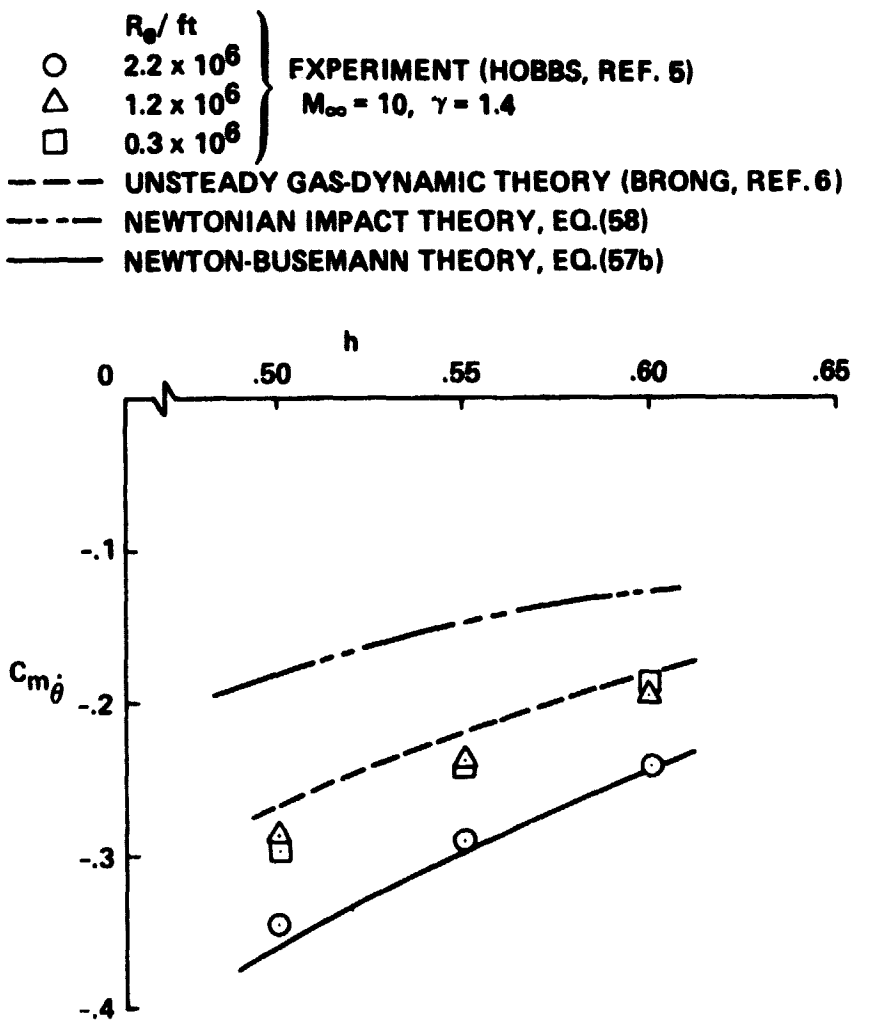
R_e/ ft
2.2 x 10^6
1.2 x 10^6
0.3 x 10^6
FXPERIMENT (HOBBS, REF. 5)
M_∞ = 10, γ = 1.4
UNSTEADY GAS-DYNAMIC THEORY (BRONG, REF. 6)
NEWTONIAN IMPACT THEORY, EQ.(58)
NEWTON-BUSEMANN THEORY, EQ.(57b)
h
0
.50
.55
.60
.65
-.1
-.2
-.3
-.4
$C_{m_{\dot\theta}}$

Fig. 2

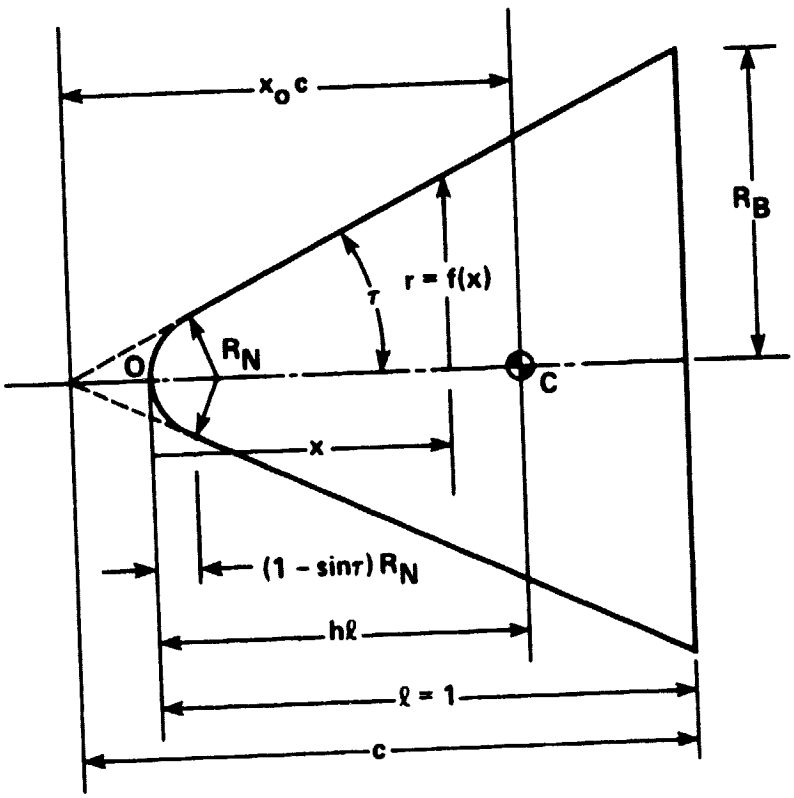

Fig. 3

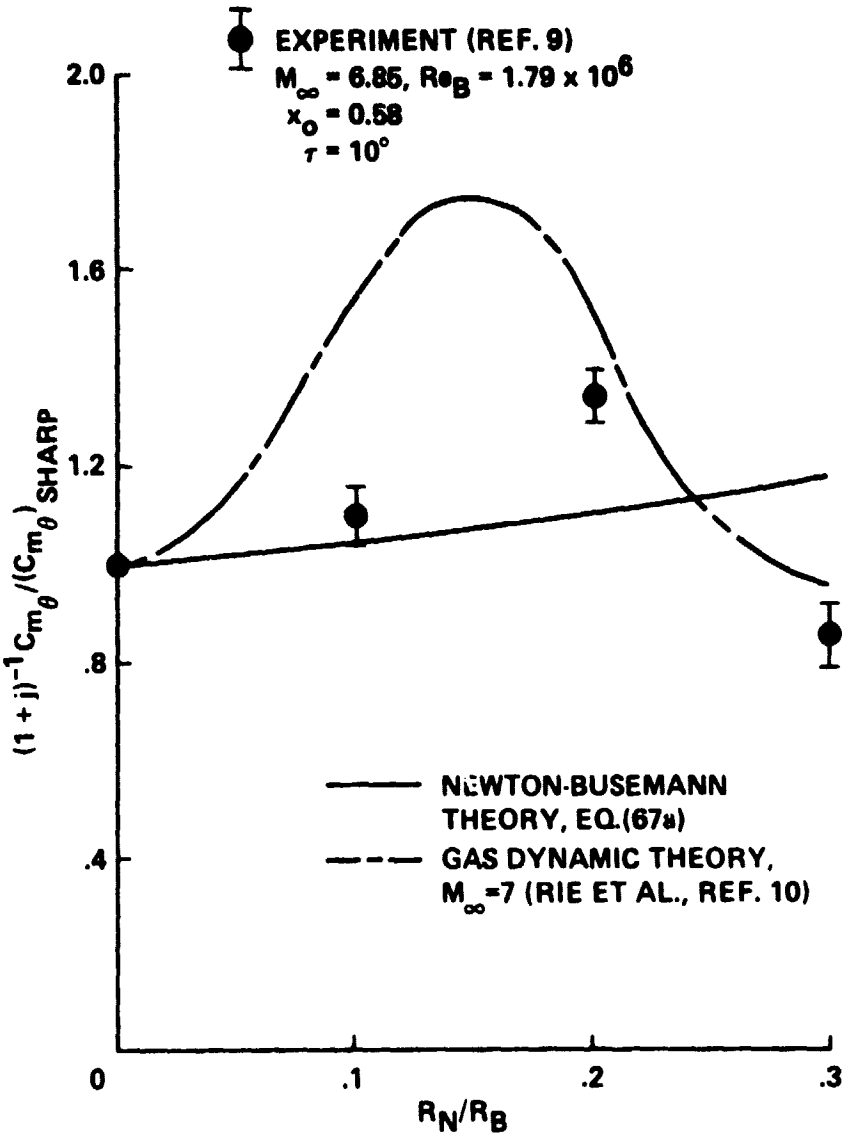
EXPERIMENT (REF. 9)
M_∞ = 6.85, Re_B = 1.79 x 10^6
x_o = 0.58
τ = 10°
2.0
1.6
1.2
.8
.4
0
.1
.2
.3
$(1+j)^{-1}C_{m_\theta}/(C_{m_\theta})_{SHARP}$
R_N/R_B
NEWTON-BUSEMANN THEORY, EQ.(67a)
GAS DYNAMIC THEORY, M_∞=7 (RIE ET AL., REF. 10)

Fig. 4

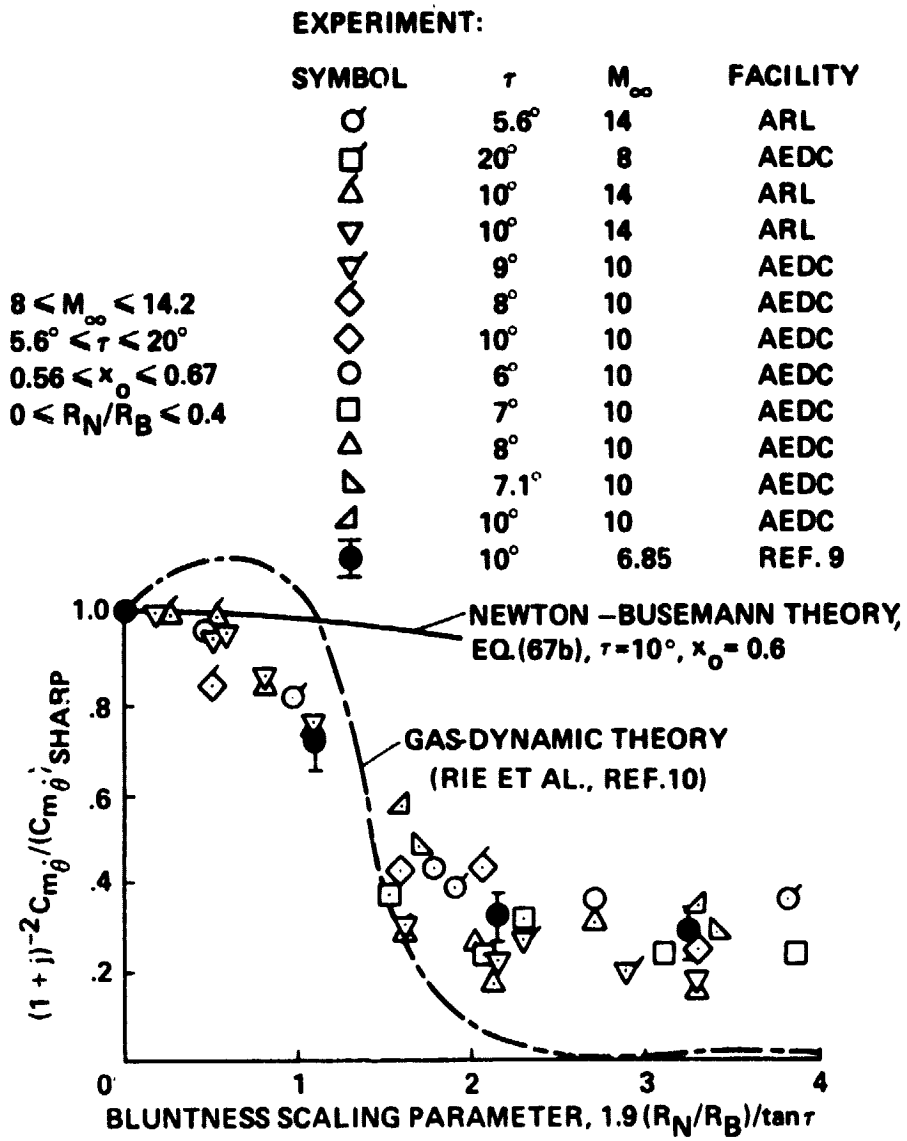
EXPERIMENT:
SYMBOL τ M∞ FACILITY
5.6° 14 ARL
20° 8 AEDC
10° 14 ARL
10° 14 ARL
9° 10 AEDC
8° 10 AEDC
10° 10 AEDC
6° 10 AEDC
7° 10 AEDC
8° 10 AEDC
7.1° 10 AEDC
10° 10 AEDC
10° 6.85 REF. 9
8 ≤ M∞ ≤ 14.2
5.6° ≤ τ ≤ 20°
0.56 ≤ x0 ≤ 0.67
0 ≤ RN/RB ≤ 0.4
NEWTON –BUSEMANN THEORY, EQ.(67b), τ=10°, x0= 0.6
GAS-DYNAMIC THEORY (RIE ET AL., REF.10)
(1 + j)^-2 Cmθ/(Cmθ)'SHARP
1.0
.8
.6
.4
.2
0
1
2
3
4
BLUNTNESS SCALING PARAMETER, 1.9 (RN/RB)/tanτ

Fig. 5

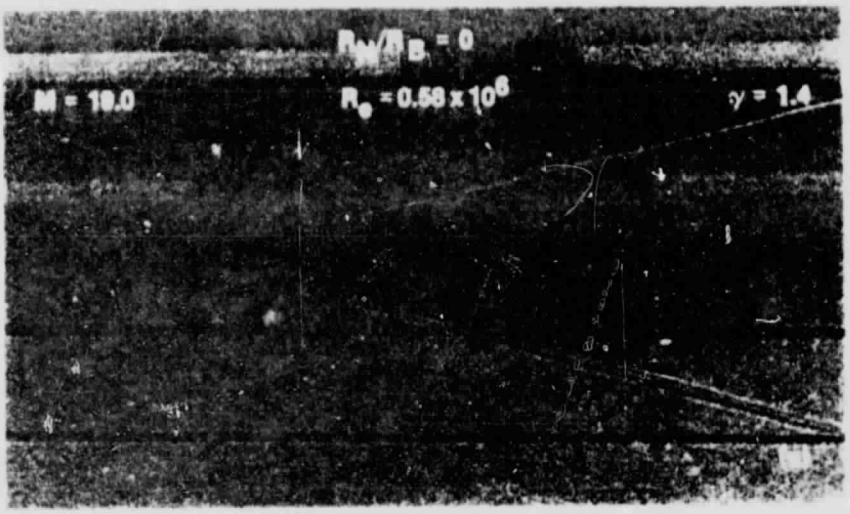

Fig. 6a

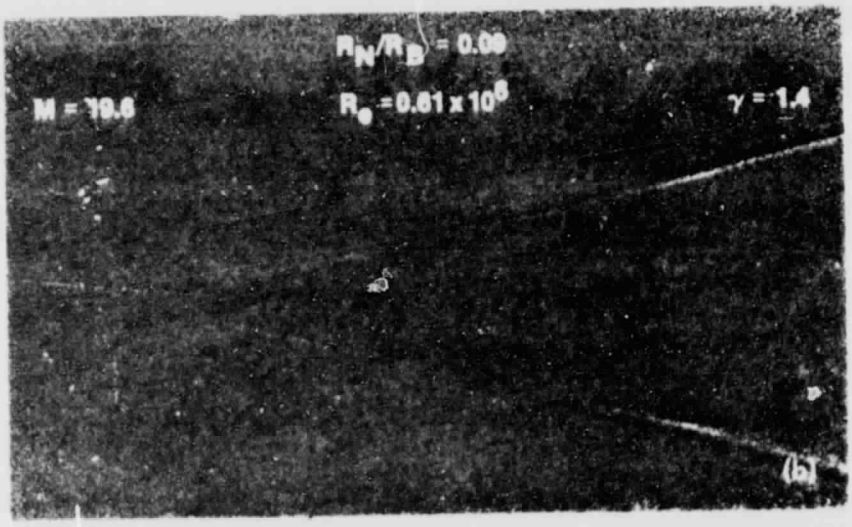

Fig. 6b

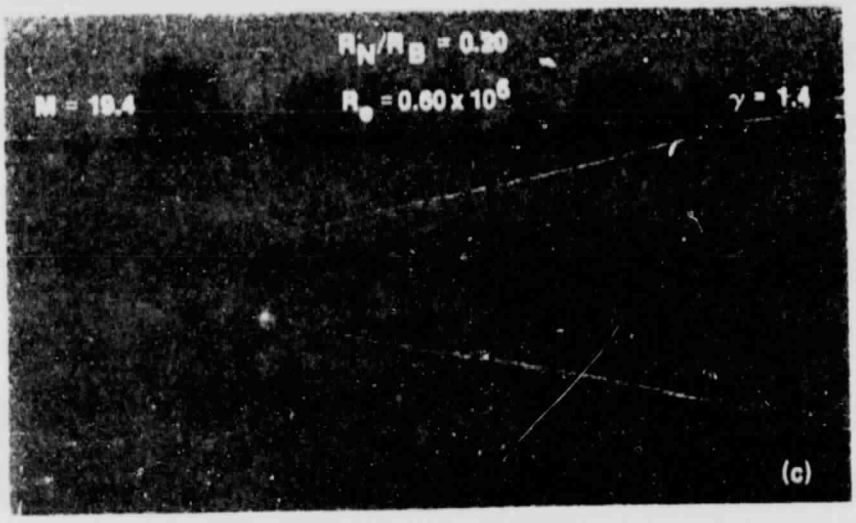

Fig. 6c

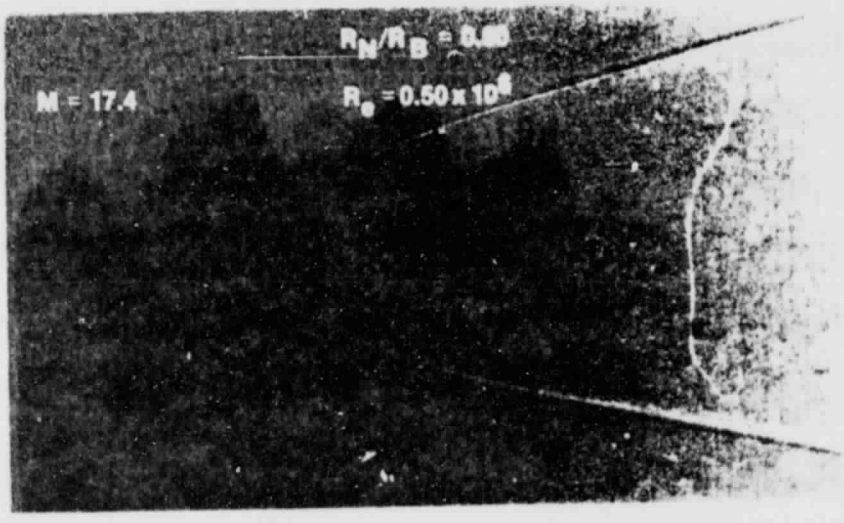

Fig. 6d

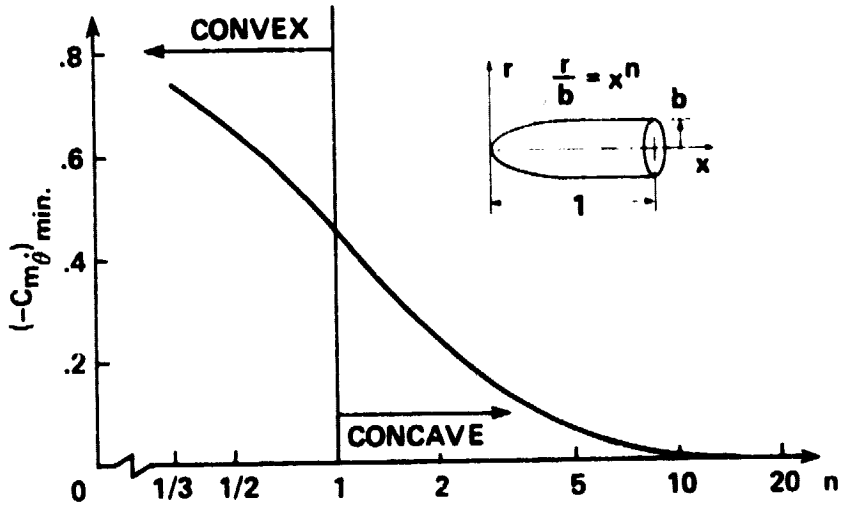
CONVEX
CONCAVE
$(-C_{m_{\dot{\theta}}})_{min.}$
.8
.6
.4
.2
0
1/3
1/2
1
2
5
10
20
n
r
$\frac{r}{b} = x^n$
b
x
1

Fig. 7